

Three-body approach to the atomic reactions of electron transfer: II. Calculation of total cross sections

G V Avakov[†], A R Ashurov[‡], L D Blokhintsev[†], A S Kadyrov[†],
A M Mukhamedzhanov[‡] and M V Poletayeva[†]

[†] Institute of Nuclear Physics, Moscow State University, Moscow 119899, USSR

[‡] Institute of Nuclear Physics, Uzbek Academy of Sciences, Tashkent, USSR

Received 18 May 1989, in final form 5 June 1990

Abstract. The previous paper proposed an approach to the calculation of electron transfer reactions in ion–atomic collisions based on the Alt–Grassberger–Sandhas three-body equations for the purely Coulomb interaction. In the present paper the equations derived in I are solved numerically for concrete charge-exchange reactions. The effective potential of the problem is taken in its lowest order approximation which corresponds to the ‘pole’ electron transfer amplitude. The total and partial cross sections and a few other characteristics of the reactions $H^+ + H \rightarrow H + H^+$, $H^+ + He(1s^2) \rightarrow H + He^+(1s)$, $He^{2+} + H \rightarrow He^+ + H^+$ and $Li^{3+} + H \rightarrow Li^{2+} + H^+$ are calculated in a wide range of collision energies from 0.1–100 keV amu^{−1}.

1. Introduction

In the previous paper (Avakov *et al* 1990, hereafter referred to as I) we developed an approach to the calculation of electron transfer reactions in ion–atomic collisions based on the Faddeev three-body equations written in the Alt–Grassberger–Sandhas (AGS) form for the purely Coulomb interaction in the impact parameter representation (hereafter referred to as the impact parameter Faddeev approach (IPFA)). Here we solve numerically the equations derived in I, in the case of concrete charge-exchange reactions. In section 2 the equations are used to calculate electron transfer reactions without the ‘optical’ Coulomb interaction between heavy fragments (where one fragment is a neutral atom). The cross sections for the reactions $H^+ + H \rightarrow H + H^+$ and $H^+ + He(1s^2) \rightarrow H + He^+(1s)$ are calculated. In section 3 the developed approach is used to calculate reactions with the ‘optical’ Coulomb interaction in the outgoing channel. As an example, we calculate the pick-up cross sections of the electron by fully stripped He^{2+} and Li^{3+} ions in collisions with hydrogen atoms. Section 4 summarizes the results and presents concluding remarks.

The notations used here are the same as in I.

2. Calculations in the absence of the ‘optical’ Coulomb interaction

2.1. Reaction $H^+ + H(1s) \rightarrow H + H^+$

In the system (55) of I the number of equations used to calculate the amplitude \tilde{T}_{nlm} numerically, depends on the maximum principal quantum number n_{\max} in the set of

quantum numbers $r = (n, l, m)$ which ensures the required accuracy of the cross section calculations[†]. At a fixed n_{\max} the number of equations in the system is equal to $\frac{1}{6}n_{\max}(n_{\max} + 1)(2n_{\max} + 1)$. The total cross section for electron transfer to the final state with quantum numbers n, l, m is determined by the known expression

$$\sigma_{nlm} = 2\pi \int_0^\infty d\rho \rho P_{nlm}(\rho) \quad (1)$$

where the transition probability at a fixed value of the impact parameter ρ , $P_{nlm}(\rho)$ is related to the amplitude $\tilde{T}_{nlm}(\rho)$ by the relation:

$$P_{nlm}(\rho) = \frac{1}{(2\pi v)^2} |\tilde{T}_{nlm}(\rho)|^2. \quad (2)$$

Table 1 lists the values of the total cross sections for the reactions $H^+ + H(1s) \rightarrow H + H^+$, $\sigma = \sum_{nlm} \sigma_{nlm}$ calculated in IPFA at $n_{\max} = 1-5$. It is seen that up to collision energies of a few keV the inclusion of only one lowest state ensures a very good accuracy for $\sigma(E)$.

The total cross section $\sigma(E)$ is shown in figure 1 in comparison with the experimental data. Here is also given the cross section calculated in the Brinkmann-Kramers approximation. At energies of tens of keV and upward the theoretical cross section is larger than the experimental. This, in particular, is accounted for in that the theoretical curve was calculated in the lowest (pole) approximation in the effective potential. Allowance for the higher-order terms of the quasi-Born expansion (25) from I should give a decrease in the theoretical cross section. An example of such a calculation

Table 1. Total cross section for the reaction $H^+ + H(1s) \rightarrow H + H^+$, $\sigma(E)$ (10^{-16} cm²) calculated at different values of n_{\max} .

E (keV)	n_{\max}				
	1	2	3	4	5
1-1	2.64+1	2.64+1	2.64+1	2.64+1	2.64+1
2-1	2.48+1	2.48+1	2.48+1	2.48+1	2.48+1
4-1	2.31+1	2.31+1	2.31+1	2.31+1	2.31+1
6-1	2.21+1	2.21+1	2.21+1	2.21+1	2.21+1
1	2.07+1	2.07+1	2.07+1	2.07+1	2.07+1
2	1.87+1	1.87+1	1.87+1	1.87+1	1.87+1
4	1.63+1	1.61+1	1.63+1	1.63+1	1.63+1
6	1.46+1	1.41+1	1.43+1	1.43+1	1.44+1
1+1	1.22+1	1.10+1	1.10+1	1.11+1	1.11+1
2+1	8.00	7.15	6.79	6.68	6.64
4+1	3.43	3.81	3.78	3.75	3.72
6+1	1.48	1.83	1.91	1.94	1.96
1+2	3.35-1	4.29-1	4.61-1	4.74-1	4.81-1
2+2	2.31-2	2.85-2	3.03-2	3.11-2	3.15-2
4+2	9.03-4	1.07-3	1.12-3	1.14-3	1.15-3
6+2	1.12-4	1.30-4	1.36-4	1.39-4	1.40-4

[†] In what follows, in solving the system (55) of I the maximum principal quantum number in the set of quantum numbers r' is also set equal to n_{\max} .

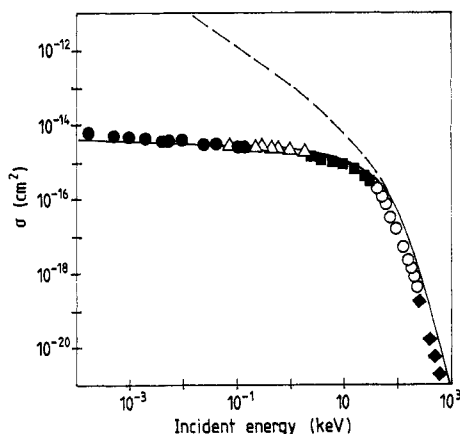


Figure 1. Total cross sections for the process $H^+ + H(1s) \rightarrow H + H^+$. Theory: full curve, IPFA; broken curve, Brinkmann-Kramers calculation. Experiment: ●, Newman *et al* (1982); △, Fite *et al* (1962); ■, McClure (1966); ○, Wittkower *et al* (1966); ◆, Hvelplund and Anderson (1982).

allowing for the $1s \rightarrow 1s$ transition only is the calculation made of Chaudhuri *et al* (1973). Besides, the three-particle break-up channel, which provides the dominant contribution at high energies, can be allowed for in higher terms of the quasi-Born expansion.

The total transition probability $P(\rho)$ as a function of the impact parameter at different collision energies is shown in figure 2. This figure illustrates the statement that, at higher energies, the contribution to the cross section is provided by the region of smaller impact parameters. The positions of maxima of the function $P(\rho)$ at low energies are determined by the values of the impact parameter $\rho \sim R_0$, where R_0 is the distance between colliding nuclei at which the molecular bonds get 'switched on'. The distance R_0 decreases as the collision velocity increases.

Figure 3 presents the partial cross sections for electron capture from the $1s$ state of the hydrogen atom to states of the hydrogen atom with principal quantum number n , $\sigma_n = \sum_{lm} \sigma_{nlm}$ at different collision energies. It is seen from this figure that at all the

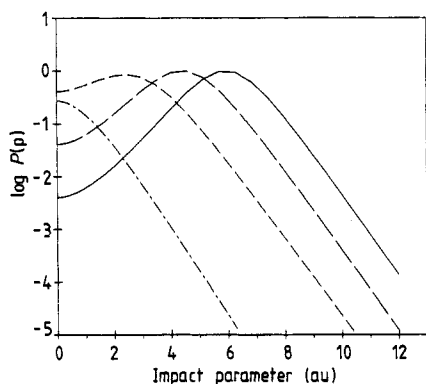


Figure 2. Total probability $P(\rho)$ of the transition $H^+ + H(1s) \rightarrow H + H^+$ as a function of the impact parameter ρ at collision energies: full curve $E = 0.1$ keV; long broken curve, $E = 1.0$ keV; short broken curve, $E = 10$ keV; chain curve, $E = 100$ keV.

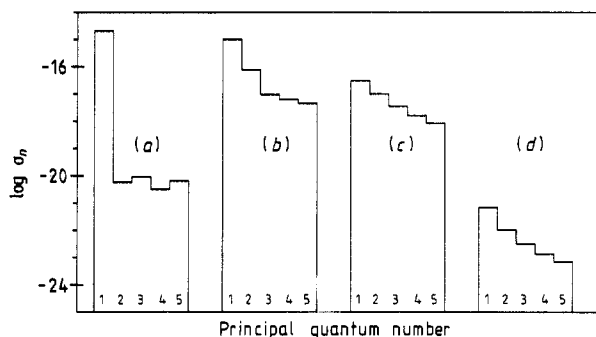


Figure 3. Partial cross section σ_n for the process $\text{H}^+ + \text{H}(1s) \rightarrow \text{H} + \text{H}^+$ plotted against the principal quantum number n of the final state at collision energies: (a) $E = 1$ keV; (b) $E = 10$ keV; (c) $E = 100$ keV; (d) $E = 1000$ keV.

energies the maximum cross section is the cross section for electron transfer from the ground to ground state of the hydrogen atom, and as the principal quantum number of the final state increases, the partial cross section rapidly decreases.

Note that in figure 3(a) (low energies) one can see two minima for σ_2 and σ_4 whose origin is not clear to us. In the high energy region the histograms are smoothed out, approaching the n^{-3} law.

Table 2 gives the partial cross sections for the reaction $\text{H}^+ + \text{H}(1s) \rightarrow \text{H} + \text{H}^+$, σ_{nlm} at five values of the collision energy from 0.1 to 10^3 keV. It is seen that at sufficiently high energies the main contribution to the total cross section is also provided by σ_{100} .

One can also see from table 2 that the transitions to s states provide the largest contribution in the medium and high energy region at fixed n (an exception is σ_{520} at $E = 10$ keV).

Figure 4 shows IPFA partial cross section for the electron capture into the 2s state of the hydrogen atom, $\text{H}^+ + \text{H}(1s) \rightarrow \text{H}(2s) + \text{H}^+$ and, for comparison, the experimental results of different groups and the theoretical curves from the paper of Cheshire *et al* (1970). It is seen that at the peak and in the high-energy region the values calculated in IPFA are higher than the experimental cross sections.

This discrepancy between our calculations and experiment can arise from the fact that the partial cross section calculations are more sensitive to the approximations used, as compared with the total cross section calculations.

2.2. Reaction $\text{H}^+ + \text{He}(1s^2) \rightarrow \text{H} + \text{He}^+(1s)$

Consider the electron transfer process



when the Coulomb interaction between heavy fragments is absent. Strictly speaking, this reaction cross section should be calculated in the framework of a four-body problem (proton, α -particle and two electrons). In the present paper the reaction (3) cross section is calculated in the three-body model in which the basic particles are the proton, the He^+ ion and the electron, i.e. in this model He^+ is considered as an inert core (the electron in He^+ is assumed to be always in the 1s state). The bound states of the second (transferred) electron are approximately described by hydrogen-like

Table 2. Partial cross sections for the reaction $H^+ + H(1s) \rightarrow H + H^+$ σ_{nlm} (10^{-16} cm^2).

$nl m $	E (keV)				
	0.1	1	10	100	1000
100	2.64+1	2.07+1	1.01+1	3.18-1	7.01-6
200	6.38-11	9.68-6	6.08-1	5.68-2	9.61-7
210	8.24-12	3.11-5	9.56-2	3.76-2	6.83-8
211	9.16-14	8.46-6	2.90-2	3.86-3	5.83-9
300	3.51-13	2.55-6	5.29-2	1.80-2	2.90-7
310	5.84-11	1.87-5	2.91-3	1.37-2	2.43-8
311	5.92-14	2.49-6	6.20-3	1.33-3	2.06-9
320	4.24-12	6.41-5	2.06-2	1.06-3	2.41-10
321	3.21-13	1.73-7	2.54-3	2.52-4	5.17-11
322	5.14-17	1.52-7	5.80-4	1.96-5	3.73-12
400	1.13-14	4.10-7	1.04-2	7.75-3	1.23-7
410	9.79-12	3.14-7	1.29-3	6.17-3	1.09-8
411	9.74-15	3.91-8	2.83-3	5.90-4	9.19-10
420	1.23-13	2.10-5	2.47-2	6.36-4	1.45-10
421	4.61-14	2.37-6	2.38-3	1.49-4	3.11-11
422	4.64-17	1.74-7	3.30-4	1.14-5	2.24-12
430	7.31-13	2.08-6	1.47-2	1.57-5	4.85-13
431	2.40-15	1.15-6	5.00-4	6.05-6	1.75-13
432	3.36-16	4.16-7	6.90-5	9.92-7	2.73-14
433	2.22-18	6.57-9	7.07-6	6.48-8	1.72-15
500	5.71-12	1.28-6	3.54-3	4.01-3	6.31-8
510	1.78-12	4.25-5	1.05-3	3.25-3	5.72-9
511	6.35-15	6.64-7	1.54-3	3.08-4	4.82-10
520	1.56-11	1.75-6	1.78-2	3.73-4	8.54-11
521	1.87-15	2.29-6	1.62-3	8.69-5	1.83-11
522	1.60-17	4.94-7	1.89-4	6.62-6	1.31-12
530	1.94-12	7.29-6	1.33-2	1.34-5	4.17-13
531	2.62-15	2.34-6	4.58-4	5.13-6	1.50-13
532	1.53-16	5.19-8	5.95-5	8.36-7	2.34-14
533	8.01-19	3.32-8	5.51-6	5.43-8	1.47-15
540	2.73-13	4.00-7	1.62-3	1.53-7	6.59-16
541	5.69-14	1.69-7	1.98-5	7.89-8	3.27-16
542	2.04-18	9.07-9	2.93-6	2.00-8	8.00-17
543	9.83-18	3.74-10	5.82-7	2.66-9	1.04-17
544	1.57-20	1.37-10	3.81-8	1.52-10	5.80-19

wavefunctions with effective charges. The effective charge for the $n = 1$ ground state was set equal to 1.6875 and for $n > 1$ the effective charges were taken from Slater (1930). The reaction (3) total cross section calculated in IPFA is shown in figure 5 in comparison with the available experimental data. Here is also given the cross section obtained in the so-called unitarized distorted wave approximation (UDWA) (Suzuki *et al* 1984), in the boundary-corrected first Born approximation (Decker and Eichler 1989) and in the normalized Brinkmann-Kramers approximation (Shevelko 1981). At energies $E > 20 \text{ keV amu}^{-1}$ our cross section is larger than the experimental values, as in the case of the reaction $H^+ + H \rightarrow H + H^+$. However, at lower energies it agrees better with experiment than do the UDWA calculations.

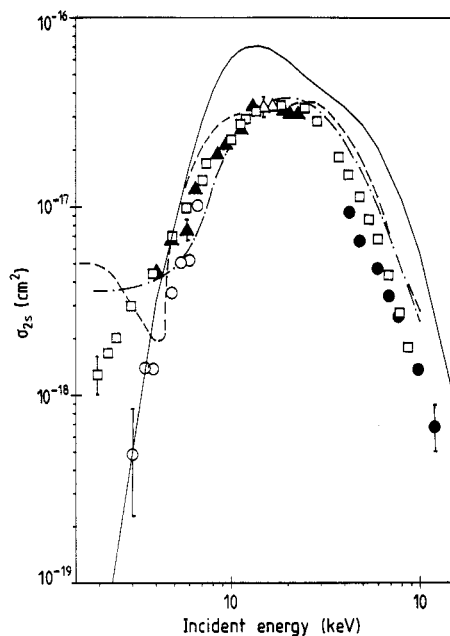


Figure 4. Partial cross section σ_{2s} for the process $H^+ + H(1s) \rightarrow H(2s) + H^+$. Theory: full curve, IPFA; broken curve, four-state hydrogenic close coupling; chain curve, seven-state hydrogenic close coupling (Cheshire *et al* 1970). Experiment: \square , Toburen *et al* (1968); \circ , Bayfield (1969); \blacktriangle , Stedford and Hasted (1955); \bullet , Stier and Barnett (1956); \triangle , Welsh *et al* (1967).

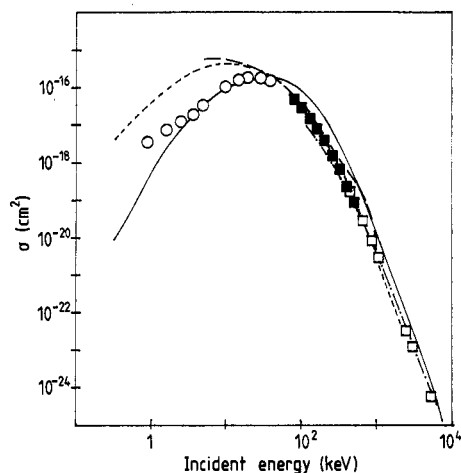


Figure 5. Total cross section for the process $H^+ + He(1s^2) \rightarrow H + He^+(1s)$. Theory: full curve, IPFA; broken curve, UDWA (Suzuki *et al* 1984); dotted curve, normalized Brinkmann-Kramers approximation (Shevelko 1981); chain curve, boundary-corrected first Born approximation (Decker and Eichler 1989). Experiment: \circ , Stedford and Hasted (1955); \blacksquare , Shah and Gilbody (1985); \square , Welsh *et al* (1967).

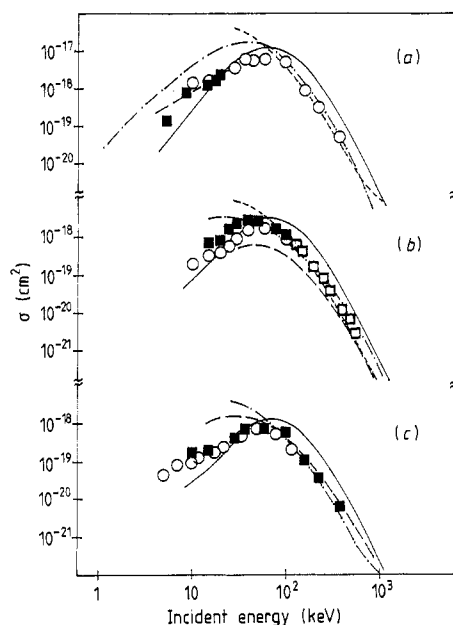


Figure 6. Partial cross sections for the process $\text{H}^+ + \text{He}(1s^2) \rightarrow \text{H} + \text{He}^+(1s)$. (a) Cross section σ_{2s} . Theory: full curve, IPFA; dotted curve, Belkić and Gayet (1977); broken curve, Kimura (1985); chain curve, Shevelko (1980). Experiment: ■, Fitzwilson and Thomas (1971); ○, Rodbro and Anderson (1979). (b) Cross section σ_{3s} . Theory: full curve, IPFA; dotted curve, Belkić and Gayet (1977); broken curve, Deco *et al* (1984); chain curve, Winter and Lin (1974). Experiment: ○, Hughes *et al* (1970); ■, Lenormand (1976); □, Ford and Thomas (1972). (c) Cross section σ_{4s} . Theory: full curve, IPFA; chain curve, Belkić and Gayet (1977); broken curve, Winter and Lin (1974). Experiment: ○, Hughes *et al* (1967); ■, Rodbro and Andersen (1979).

Figure 6 shows the theoretical and experimental partial cross sections for electron capture into 2s, 3s and 4s states of the H atom within collision energies of 10–10³ keV. Just as in the case of the total cross section, IPFA satisfactorily describes the low-energy region and the peak and demonstrates that the theoretical values are higher than the experimental at high energies.

Calculations of the reaction (3) cross section show, first, that our approach can be extended to more complex particle systems and, second, that an approximate, hydrogen-like wavefunction for the He atom might be used in certain cases.

3. Charge-exchange reactions with the ‘optical’ Coulomb interaction

3.1. Reaction $\text{He}^{2+} + \text{H}(1s) \rightarrow \text{He}^+ + \text{H}^+$

This process was studied in many theoretical and experimental papers. The measured total cross sections are often very different in value.

Table 3 lists the calculated values of the total cross sections for the reaction $\text{He}^{2+} + \text{H} \rightarrow \text{He}^+ + \text{H}^+$ at $n_{\text{max}} = 1-5$. It is seen that at $n_{\text{max}} = 5$ the accuracy of calculation of $\sigma(E)$ is sufficiently good within the whole energy range under study. The total theoretical cross section $\sigma(E)$ is shown in figure 7 in comparison with experiment and

Table 3. Total cross section for the reaction $\text{He}^{2+} + \text{H}(1s) \rightarrow \text{He}^+ + \text{H}^+ \sigma(E) (10^{-16} \text{ cm}^2)$ calculated at different values of n_{max} .

$E \text{ (keV amu}^{-1}\text{)}$	n_{max}				
	1	2	3	4	5
1-1	5.63-4	5.63-4	5.63-4	5.63-4	5.63-4
2-1	1.52-3	1.54-3	1.54-3	1.54-3	1.54-3
4-1	3.83-3	3.65-2	3.66-2	3.65-2	3.65-2
6-1	7.10-3	5.90-1	5.90-1	5.90-1	5.90-1
1	1.73-2	6.74	6.75	6.75	6.75
2	5.80-2	2.74+1	2.76+1	2.76+1	2.76+1
4	1.81-1	3.14+1	3.20+1	3.21+1	3.21+1
6	3.25-1	2.85+1	2.95+1	2.96+1	2.97+1
1+1	5.93-1	2.32+1	2.46+1	2.45+1	2.45+1
2+1	9.79-1	1.52+1	1.62+1	1.66+1	1.67+1
4+1	1.04	8.10	9.07	9.14	9.11
6+1	8.37-1	4.44	5.54	5.90	6.05
1+2	4.50-1	1.48	1.93	2.14	2.25
2+2	9.32-2	1.84-1	2.25-1	2.43-1	2.54-1
4+2	8.35-3	1.22-2	1.37-2	1.44-2	1.48-2
6+2	1.47-3	1.95-3	2.13-3	2.20-3	2.24-3

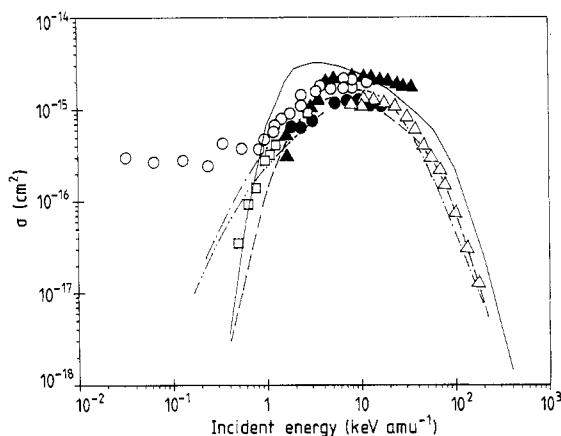


Figure 7. Total cross section for the process $\text{He}^{2+} + \text{H}(1s) \rightarrow \text{He}^+ + \text{H}^+$. Theory: full curve, IPFA; broken curve UDWA (Ryufuku and Watanabe 1978); chain curve, Fujiwara and Toshima (1983) (atomic orbital close coupling); chain curve, Winter and Lane (1978) (molecular orbital close coupling). Experiment: \circ , Fite *et al* (1962); \blacktriangle , Bayfield and Khayrallah (1975); \square , Nutt *et al* (1978); \bullet , Shah and Gilbody (1974); \triangle , Olson *et al* (1977).

theoretical results of other groups. It is seen from this figure that at $E > 1 \text{ keV amu}^{-1}$ the cross section calculated in IPFA is larger than the measured cross section. To improve the agreement of the theory with experiment, it is necessary to include the higher order terms for the effective potential.

The total transition probability $P(\rho)$ as an impact-parameter function at different collision energies is shown in figure 8. In the low energy region the curves $P(\rho)$ are

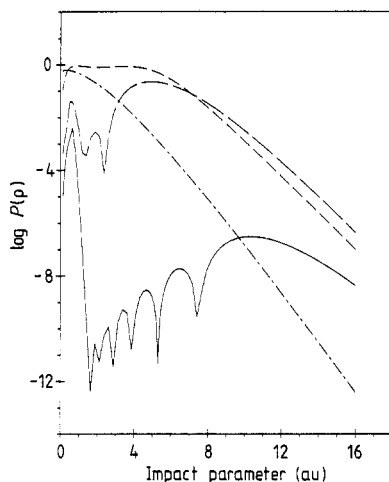


Figure 8. Total probability $P(\rho)$ of the transition $\text{He}^{2+} + \text{H}(1s) \rightarrow \text{He}^+ + \text{H}^+$ plotted against the impact parameter at collision energies: full curve, $E = 0.2 \text{ keV amu}^{-1}$; long broken curve, $E = 1.0 \text{ keV amu}^{-1}$; short broken curve, $E = 10 \text{ keV amu}^{-1}$; chain curve, $E = 100 \text{ keV amu}^{-1}$.

of oscillating character and next they decrease rapidly at high ρ . As the collision energy increases, the region of oscillations gets narrower. A similar picture is given by the calculations made in other approaches (Ryufuku and Watanabe 1978).

The partial cross sections for electron capture from the 1s state of the H atom into the states of the hydrogen-like He^+ atom with the principal quantum number n , σ_n , at different collision energies are shown in figure 9. It is seen that in the presence of the 'optical' Coulomb interaction between He^+ and H^+ at low collision energies the dominant transition is the non-resonance transition to the state with $n = 1$ †. Within the approximations used, this can be explained by the fact that equations (64)–(66) in I for the effective potentials $\tilde{V}_{\beta,\alpha}^{(0)}(\rho)$ contain the factor

$$\exp\left(-\eta \tan^{-1} \frac{2\varepsilon_\alpha - 2\varepsilon_\beta + v^2(1 - 2\alpha)}{2v\chi}\right)$$

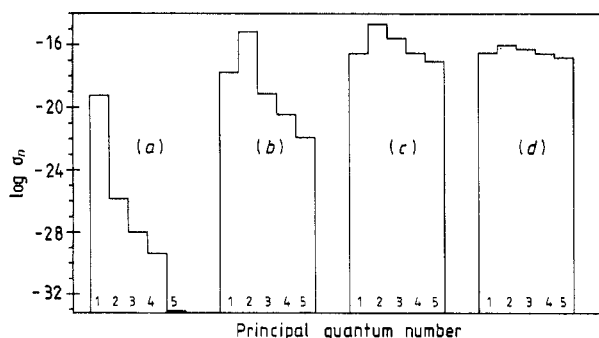


Figure 9. Partial cross section σ_n for the process $\text{He}^{2+} + \text{H}(1s) \rightarrow \text{He}^+ + \text{H}^+$ plotted against the principal quantum number n of the final state at collision energies: (a) $E = 0.1 \text{ keV amu}^{-1}$; (b) $E = 1.0 \text{ keV amu}^{-1}$; (c) $E = 10 \text{ keV amu}^{-1}$; (d) $E = 100 \text{ keV amu}^{-1}$.

† This result disagrees with the experimental data of Afrosimov *et al* (1988).

which can become rather large at $\varepsilon_\beta > \varepsilon_\alpha$ and compensate the exponential decrease of the Bessel functions of the third kind with increasing argument. At higher energies the $n=2$ state transition is dominant.

Table 4 presents the partial cross sections σ_{nlm} at four collision energies in the interval of 0.1 to 100 keV amu⁻¹.

3.2. Reaction $\text{Li}^{3+} + \text{H}(1s) \rightarrow \text{Li}^{2+} + \text{H}^+$

The total cross section for the reaction $\text{Li}^{3+} + \text{H}(1s) \rightarrow \text{Li}^{2+} + \text{H}^+$ calculated in IPFA, is plotted as a collision energy function in figure 10. Here are also shown, for comparison, the experimental and theoretical results of other groups. Our cross section closely

Table 4. Partial cross sections for the reaction $\text{He}^{2+} + \text{H}(1s) \rightarrow \text{He}^+ + \text{H}$ $\sigma_{nlm}(10^{-16} \text{ cm}^2)$.

$nl m $	$E \text{ (keV amu}^{-1}\text{)}$			
	0.1	1	10	100
100	5.63-4	1.73-2	2.90-1	3.16-1
200	6.45-11	2.81	5.02	7.99-2
210	1.05-13	9.96-2	6.92	6.41-1
211	3.70-11	1.91	4.67	1.27-1
300	5.39-13	2.01-5	1.47-1	2.78-2
310	4.14-13	2.55-4	6.96-1	2.35-1
311	1.52-14	9.84-6	2.13-1	3.83-2
320	3.38-14	6.67-6	8.53-1	1.10-1
321	2.26-15	1.08-4	1.92-1	3.72-2
322	3.70-17	1.04-4	4.13-2	3.82-3
400	2.71-14	1.36-5	3.53-3	1.24-2
410	1.29-14	2.67-6	1.11-1	1.06-1
411	4.27-16	1.88-6	1.86-2	1.62-2
420	1.17-15	1.16-6	6.23-2	6.30-2
421	6.87-17	1.20-6	1.21-2	2.02-2
422	1.03-18	8.22-7	5.05-3	1.96-3
430	2.96-17	4.48-7	1.40-2	7.91-3
431	2.20-18	9.32-7	1.34-2	3.75-3
432	5.23-20	3.37-6	1.64-3	7.37-4
433	5.02-22	1.12-6	7.27-4	5.58-5
500	3.61-18	3.98-7	3.51-3	6.52-3
510	3.27-18	3.28-8	2.82-2	5.61-2
511	8.55-20	3.31-8	3.41-3	8.28-3
520	5.83-19	3.43-8	8.06-3	3.62-2
521	2.45-20	1.11-8	1.57-3	1.13-2
522	2.55-22	9.29-9	1.33-3	1.07-3
530	4.14-20	3.97-7	9.86-4	6.45-3
531	2.01-21	9.68-9	5.43-3	2.99-3
532	3.17-23	2.33-8	7.02-4	5.74-4
533	1.94-25	4.10-8	1.62-4	4.25-5
540	1.16-21	1.22-7	2.01-3	3.44-4
541	5.87-23	1.17-8	8.12-3	2.02-4
542	1.05-24	1.94-9	1.47-3	5.77-5
543	8.96-27	8.34-9	5.72-5	8.52-6
544	3.65-29	1.73-9	1.20-6	5.31-7

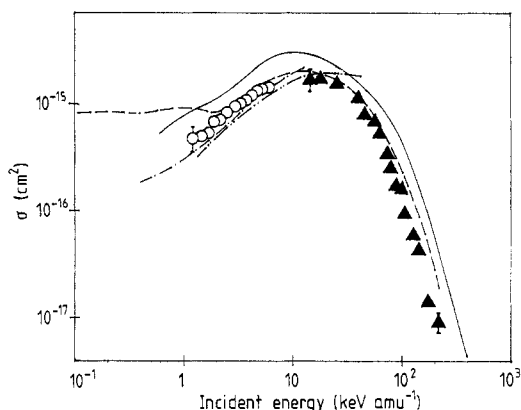


Figure 10. Total cross section for the process $\text{Li}^{3+} + \text{H}(1s) \rightarrow \text{Li}^{2+} + \text{H}^+$. Theory: full curve, IPFA; broken curve, UDWA (Ryufuku 1982); chain curve, Fritsch and Lin (1982) (atomic orbital close coupling), double chain curve, Salin (1982) (molecular orbital close coupling). Experiment: \circ , Seim *et al* (1981); \blacktriangle , Shah *et al* (1978).

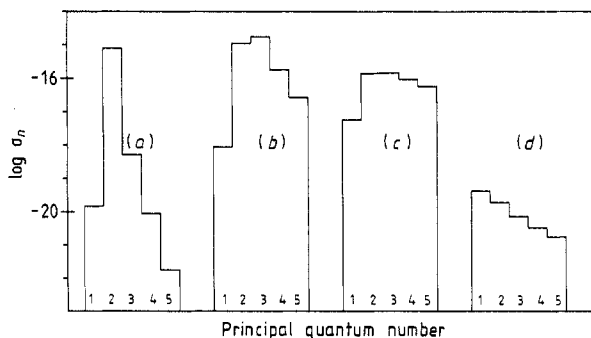


Figure 11. Partial cross section σ_n for the process $\text{Li}^{3+} + \text{H}(1s) \rightarrow \text{Li}^{2+} + \text{H}^+$ plotted against the principal quantum number n of the final state at collision energies; (a) $E = 1 \text{ keV amu}^{-1}$; (b) $E = 10 \text{ keV amu}^{-1}$; (c) $E = 100 \text{ keV amu}^{-1}$, (d) $E = 1000 \text{ keV amu}^{-1}$.

resembles the experimental cross section but it is a bit larger within the whole energy interval under examination.

Figure 11 shows the partial cross sections σ_n for electron capture to the state of the hydrogen-like Li^{2+} atom with principal quantum number n at different collision energies. Table 5 lists the values of the partial cross sections σ_{nlm} calculated in our model at $E = 1, 10, 100$ and $1000 \text{ keV amu}^{-1}$.

4. Conclusion

The previous paper I and the present paper employ the AGS three-body equations, modified for the case of the Coulomb interaction, to study electron transfer processes in ion-atomic collisions. To do this: (i) the AGS equations are written in the first-order K -matrix approximation, i.e. the free two-particle propagator is replaced by the corresponding delta function; (ii) the impact parameter representation is used instead of the partial-wave expansion. As a result, a system of algebraic equations for electron

Table 5. Partial cross sections for the reaction $\text{Li}^{3+} + \text{H}(1s) \rightarrow \text{Li}^{2+} + \text{H}^+$ $\sigma_{nlm}(10^{-16} \text{ cm}^2)$.

$nl m $	$E \text{ (keV amu}^{-1}\text{)}$			
	1	10	100	1000
100	1.48-4	8.72-3	5.68-2	4.14-4
200	4.35-1	2.20	1.34-1	1.01-4
210	4.18	2.60	5.85-1	7.08-5
211	1.61	3.15	3.37-1	7.45-6
300	6.37-4	7.71-1	5.82-2	3.41-5
310	1.42-3	2.78	1.62-1	2.79-5
311	7.15-4	1.83	6.64-2	2.74-6
320	6.53-4	1.22	4.79-1	2.54-6
321	2.80-4	2.55	2.58-1	6.08-7
322	1.74-4	1.91	4.14-2	4.80-8
400	4.22-6	2.82-2	2.83-2	1.51-5
410	2.70-5	1.21-1	7.01-2	1.29-5
411	6.95-6	6.42-2	2.49-2	1.24-6
420	1.97-5	2.90-2	2.30-1	1.57-6
421	7.57-6	4.38-2	1.13-1	3.68-7
422	7.41-7	6.15-2	1.62-2	2.85-8
430	3.06-6	4.20-1	1.10-1	4.77-8
431	1.40-6	3.00-1	6.65-2	1.83-8
432	2.31-7	1.10-1	1.73-2	3.03-9
433	1.39-8	1.38-3	1.68-3	2.00-10
500	3.04-8	4.75-3	1.54-2	7.91-6
510	2.48-7	1.52-2	3.66-2	6.91-6
511	2.45-7	5.98-3	1.21-2	6.54-7
520	1.87-7	6.01-3	1.24-1	9.36-7
521	2.48-7	4.89-3	5.75-2	2.17-7
522	3.80-8	5.23-3	7.81-3	1.66-8
530	3.85-8	4.89-2	7.89-2	4.12-8
531	5.98-8	2.98-2	4.62-2	1.57-8
532	1.66-8	1.32-2	1.15-2	2.57-9
533	1.15-9	1.57-4	1.06-3	1.69-10
540	3.19-9	3.29-2	1.31-2	5.88-10
541	3.72-9	1.44-2	8.82-3	3.04-10
542	1.47-9	3.83-3	3.04-3	7.73-11
543	2.07-10	1.03-4	5.36-4	1.04-11
544	1.32-11	6.61-4	3.91-5	5.98-13

transfer amplitudes and scattering amplitudes in ion-atomic collisions is obtained in the impact parameter representation. The amplitudes of these processes satisfy the two-body unitarity conditions. In the concrete calculations of charge-exchange processes the effective potential of the problem was taken in its lowest-order approximation which corresponds to the 'pole' electron transfer amplitude.

In the present paper we have calculated the total and partial cross sections and other characteristics of the charge-exchange reactions: $\text{H}^+ + \text{H} \rightarrow \text{H} + \text{H}^+$, $\text{H}^+ + \text{He}(1s^2) \rightarrow \text{H} + \text{He}^+(1s)$, $\text{He}^{2+} + \text{H} \rightarrow \text{He}^+ + \text{H}^+$ and $\text{Li}^{3+} + \text{H} \rightarrow \text{Li}^{2+} + \text{H}^+$. A distinctive feature of the first two reactions is the absence of the 'optical' Coulomb interaction whereas in the latter two reactions this interaction occurs in the outgoing channel. The

presence of the 'optical' Coulomb interaction essentially complicates the calculations. To simplify, a technique of approximate calculations has been developed in I.

Calculations of the total and partial cross sections show that in the developed approach it is possible to achieve good, on the whole, agreement with the available experimental data in a rather wide range of reactions and energies, if we use even the lowest-order approximation.

The theoretical results could, seemingly, be further improved, first of all, by refining the effective potentials (taking account of the high-order terms of the quasi-Born expansion) and by including the contribution of the three-particle ionization channel, which is essential at high energies. It is interesting, also, to verify the off-shell effects in the integral equations, which were neglected in the present calculations.

Acknowledgments

We would like to thank Professors V S Nikolaev and V S Senashenko and Dr N F Vorobjev for encouraging interest and helpful discussions.

References

- Afrosimov V V, Basalaev A A, Lozhkin K and Panov M H 1988 *10th Conf. on the Physics of Electronic and Atomic Collision (Uzhgorod)* Abstracts p 130
- Avakov G V, Ashurov A R, Blokhintsev L D, Mukhamedzhanov A M and Poletayeva M V 1990 *J. Phys. B: At. Mol. Opt. Phys.* **23** 2309-26
- Bayfield J E 1969 *Phys. Rev.* **182** 115-28
- Bayfield J E and Khayrallah G A 1975 *Phys. Rev. A* **12** 869-75
- Belkić Dž and Gayet R 1977 *J. Phys. B: At. Mol. Phys.* **10** 1923-32
- Chaudhuri J, Ghosh A S and Sil N C 1973 *Phys. Rev. A* **7** 1544-48
- Cheshire I M, Gallaher D F and Taylor A J 1970 *J. Phys. B: At. Mol. Phys.* **3** 813-32
- Decker F and Eichler J 1989 *Phys. Rev. A* **39** 1530-3
- Deco G R, Maitagan J M and Rivarola R D 1984 *J. Phys. B: At. Mol. Phys.* **17** L707-11
- Fite W L, Smith A C H and Stebbings R F 1962 *Proc. R. Soc. A* **268** 527-36
- Fitzwilson R L and Thomas E W 1971 *Phys. Rev. A* **3** 1305-9
- Ford J C and Thomas E W 1972 *Phys. Rev. A* **5** 1964-701
- Fritsch W and Lin C D 1982 *J. Phys. B: At. Mol. Phys.* **15** L281-7
- Fujiwara K and Toshima N 1983 *J. Phys. Soc. Jap.* **52** 4118-21
- Hughes R H, Dawson H R and Doughty B M 1967 *Phys. Rev.* **169** 166-70
- Hughes R H, Stigers C A, Doughty B M and Stokes E D 1970 *Phys. Rev. A* **1** 1424-32
- Hvelplund P and Andersen A 1982 *Phys. Scr.* **26** 375-80
- Kimura M 1985 *Phys. Rev. A* **31** 2158-61
- Lenormand J 1976 *J. Physique* **37** 699-710
- McClure G W 1966 *Phys. Rev.* **148** 47-54
- Newman J H, Cogan J D, Ziegler D L, Nitz D E, Rundel R D, Smith K A and Stebbings R F 1982 *Phys. Rev. A* **25** 2976-84
- Nutt W L, McCullough R W, Brady K, Shah M B and Gilbody H B 1978 *J. Phys. B: At. Mol. Phys.* **11** 1457-62
- Olson R E, Phaneuf R A, Meyer F W and Salop A 1977 *Phys. Rev. A* **16** 1867-72
- Rodbro M and Anderson F D 1979 *J. Phys. B: At. Mol. Phys.* **12** 2883-903
- Ryufuku H 1982 *Phys. Rev. A* **25** 720-36
- Ryufuku H and Watanabe T 1978 *Phys. Rev. A* **18** 2005-15
- Salin A 1982 *Phys. Lett. A* **91** 61-3
- Seim W, Müller A, Wirkuer-Bott I and Salzborn E 1981 *J. Phys. B: At. Mol. Phys.* **14** 3485-91
- Shah M B and Gilbody H B 1974 *J. Phys. B: At. Mol. Phys.* **7** 637-43
- 1985 *J. Phys. B: At. Mol. Phys.* **18** 899-913

- Shah M B, Goffe T V and Gilbody H B 1978 *J. Phys. B: At. Mol. Phys.* **11** L233-6
- Shevelko V P 1980 *J. Phys. B: At. Mol. Phys.* **13** L319-22
- 1981 *Fiz. (Zagreb)* **13** 185-98
- Slater J C 1930 *Phys. Rev.* **36** 57-64
- Stedeford J B H and Hasted J B 1955 *Proc. R. Soc. A* **227** 466-86
- Stier P M and Barnet C F 1956 *Phys. Rev.* **103** 896-907
- Suzuki H, Toshima N, Watanabe T and Ryufuku H 1984 *Phys. Rev. A* **29** 529-35
- Toburen L H, Nokai M Y and Langley R A 1968 *Phys. Rev.* **171** 114-22
- Welsh L M, Berkner K H, Kaplan S N and Ryle R V 1967 *Phys. Rev.* **158** 85-92
- Winter T G and Lane N F 1978 *Phys. Rev. A* **17** 66-79
- Winter T G and Lin C C 1974 *Phys. Rev. A* **10** 2141-55